JACS
JOURNAL OF THE AMERICAN CHEMICAL SOCIETY

COMMUNICATION

pubs.acs.org/JACS

A Nonclassical Dihydrogen Adduct of $S = {}^1/_2$ Fe(I)

Yunho Lee,[†,§,∥] R. Adam Kinney,[‡,∥] Brian M. Hoffman,[*,‡] and Jonas C. Peters[*,†]

[†]Division of Chemistry and Chemical Engineering, California Institute of Technology, Pasadena, California 91125, United States

[‡]Department of Chemistry, Northwestern University, 2145 Sheridan Road, Evanston, Illinois 60208, United States

Supporting Information

ABSTRACT: We have exploited the capacity of the "(SiP^{iPr}_3)Fe(I)" scaffold to accommodate additional axial ligands and characterized the mononuclear $S = {}^1/_2$ H_2 adduct complex $(SiP^{iPr}_3)Fe^I(H_2)$. EPR and ENDOR data, in the context of X-ray structural results, revealed that this complex provides a highly unusual example of an open-shell metal complex that binds dihydrogen as a ligand. The H_2 ligand at 2 K dynamically reorients within the ligand-binding pocket, tunneling among the energy minima created by strong interactions with the three Fe−P bonds.

Low-valent iron has been proposed to play a prominent role in the function of hydrogenase and nitrogenase enzymes, a hypothesis that has inspired the study of formally low-valent iron model complexes that afford access to N_2 and H_2 ligation.[1−3] Whereas model systems have historically focused on Fe(0) and Fe(II) systems in this context, the coordination chemistry of Fe(I) has more recently come into focus.[4] This is in part due to its suggested intermediacy in enzymatic hydrogenase activity. Fe(I) is a key formal oxidation state to consider for N_2 and H^+ reduction cycles, and understanding interactions between Fe(I) and N_2/H_2 is essential.

In several recent studies using a tripodal tetradenate tris(phosphino)silyl ligand XL_3 (e.g., SiP^{iPr}_3 = $[Si(o\text{-}C_6H_4P\text{-}iPr_2)_3]^-$),[3b,4] it has been established that five-coordinate iron in a trigonal-bipyramidal (TBP) geometry (XL_3Fe-L') can accommodate a terminally bonded N_2 (or CO) ligand in the axial site across three formal oxidation states ($XL_3Fe^0-N_2^-$, $XL_3Fe^I-N_2$, and $XL_3Fe^{II}-N_2^+$). It is noteworthy that the spin states of these TBP systems vary such that an $S = 0$ state is favored for Fe(0), an $S = {}^1/_2$ state for Fe(I), and an $S = 1$ state for Fe(II). These findings encouraged us to explore the affinity of dihydrogen for the axial site, particularly for the $S = {}^1/_2$ Fe(I) or $S = 1$ Fe(II) states. Whereas it is common for H_2 to occupy the same coordination site as N_2, thoroughly characterized dihydrogen adducts of open-shell complexes for transition metals remain exceptionally rare.[5,6] Oxidative addition to form a dihydride and heterolytic cleavage to form a monohydride are well-established alternatives. NMR techniques, including measurement of T_1 values and J_{HD} coupling constants, have been the methods of choice for characterizing closed-shell H_2 adducts and distinguishing between the dihydrogen/dihydride extrema on the H_2 bonding continuum.[7] Open-shell H_2 adduct complexes are not amenable to this approach because of the extreme line broadening of resonances expected for H atoms directly coordinated to a metal center with spin $S > 0$. Because the $S = {}^1/_2$ state is EPR-active, we reasoned that a combined electron paramagnetic resonance (EPR)/electron−nuclear double resonance (ENDOR) study might prove most effective in characterizing the product formed by reaction of H_2 with the $S = {}^1/_2$ Fe(I) complex. The present report provides the results of such a study and introduces an $S = {}^1/_2$ $Fe^I(H_2)$ adduct complex. Evidence for its related but cationic $S = 1$ $Fe^{II}(H_2)^+$ analogue is also provided.

Scheme 1

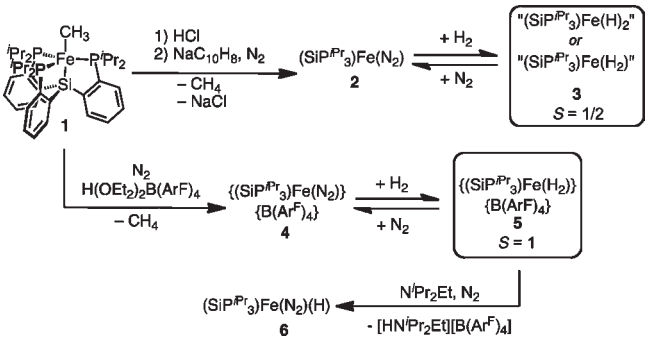

As previously reported, treatment of the methyl complex $(SiP^{iPr}_3)Fe-CH_3$ (**1**) with HCl followed by reduction generates the $S = {}^1/_2$ Fe(I)− N_2 adduct $(SiP^{iPr}_3)Fe(N_2)$ (**2**).[4a,b] The N_2 ligand is sufficiently labile to be displaced by H_2 in benzene to afford a yellow species formulated as $S = {}^1/_2$ "$(SiP^{iPr}_3)Fe(H_2)$" or "$(SiP^{iPr}_3)Fe(H)_2$" (**3**) (μ_{eff} = 1.9 μ_B by the Evans method; Scheme 1) in nearly quantitative yield. The optical spectrum of **3** [see the Supporting Information (SI)] features a low-energy d−d transition at 1350 nm ($\varepsilon \approx 100$ cm^{-1} M^{-1}) similar to that of **2** (1250 nm, $\varepsilon \approx 300$ cm^{-1} M^{-1}).

Displacement of the N_2 ligand of **2** by H_2 can be conveniently monitored by ^{1}H NMR spectroscopy in C_6D_6 (Figure 1). As shown in Figure 1, the H_2 adduct **3** is stable to vacuum over prolonged periods (even at 60 °C over 12 h) but converts back to **2** upon exposure to N_2, which would be consistent with an associative exchange process proceeding through a formally 19-electron intermediate. Alternatively, and perhaps more likely, is a process wherein a labile phosphine donor exposes a site for N_2 binding via a 15-electron intermediate, followed by H_2 loss and recoordination of the phosphine donor to provide **2**. We also prepared and similarly characterized the D_2 derivative of **3** (see the SI). The ^{1}H NMR spectrum of **3**-D_2 is analogous to that for **3**, and an ^{2}H NMR spectrum does not reveal any deuterium resonances for **3**-D_2 (see the SI). This fact is consistent with deuterons that are directly bonded to an $S = {}^1/_2$ iron center.

Received: July 26, 2011
Published: September 28, 2011

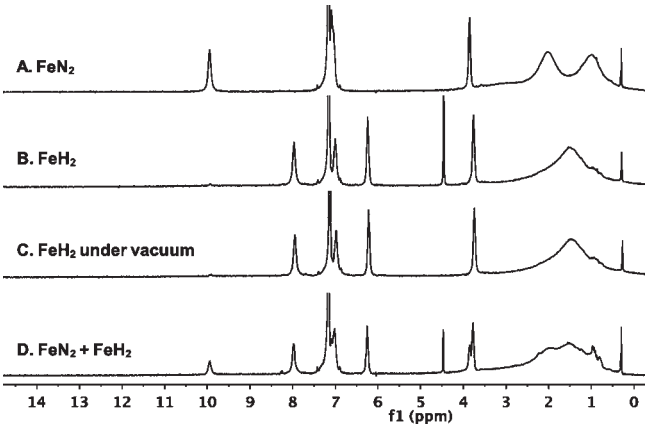

Figure 1. ^{1}H NMR spectra of (A) (SiP^{iPr}_3)Fe(N_2) (**2**), (B) (SiP^{iPr}_3)-Fe(H_2) (**3**), (C) **3** under full vacuum, and (D) a mixture of **2** and **3** measured in C_6D_6 at RT.

Incubation of **2** under HD instead of H_2 at RT for 15 h caused no $HD/H_2/D_2$ scrambling, suggesting that **3** binds an intact H_2 ligand rather than undergoing heterolytic activation (e.g., to generate a Si−H or P−H bond and an Fe−H bond).

The well-behaved NMR properties of **2** and **3** allow for the direct measurement of the equilibrium constant for H_2/N_2 exchange at the $S = {}^1/_2$ Fe center. Using sealed J-Young vessels with known N_2/H_2 gas mixtures and exploiting the well-defined resonances of the SiP^{iPr}_3 ligand at ca. 10 and 8 ppm to integrate the respective concentrations of **2** and **3**, we estimated the equilibrium constant to be 50 ± 20 in favor of H_2 binding in C_6D_6 at room temperature.

X-ray structures of **3** were obtained from crystals under vacuum and under an atmosphere of H_2. While both structures are of high quality, neither shows the positions of the H_2/hydride. Nonetheless, it is clear that the two structures are essentially identical and are likewise very similar to that of the N_2 adduct complex **2**[4b] and its CO congener (SiP^{iPr}_3)Fe^1(CO)[4c] (Figure 2 and Table 1), except for the absence of an axially bound diatomic ligand for **3**. We were unable to locate a vibration consistent with either an Fe−H or an Fe−(H−H) motif. Whereas terminal M−H vibrations are readily assigned, ν-(H−H) vibrations for H_2 adduct complexes are not as reliably discerned.[6a,7] The absence of ν(Si−H) or ν(P−H) stretches in the IR spectrum is likewise inconsistent with heterolytic generation of Fe−H and Si−H/P−H bonds but consistent with an intact H_2 ligand.

We examined the EPR spectrum of **3** in both the solid state and as a frozen glass. Treatment of **2** (**g** = [2.364, 2.036, 2.003]) with H_2 gas leads to complete loss of the starting material and the appearance of **3** with an $S = {}^1/_2$ EPR signal (**g** = [2.275, 2.064, 2.015]), as measured for frozen solutions (9:1 THF/Me-THF) and pure powders (see the SI). The unique magnetic direction $\mathbf{g}_1$ (g_1 = 2.275) is assigned to the pseudo-C_3 symmetry axis of the molecule. These low-temperature measurements of **3**, combined with NMR Evans method (Table 1) show that the coordination sphere and low-spin d^7 character of the Fe(I) center are maintained under all conditions.

The g values of **3** (and **2**) can be described in terms of a "pseudo-Jahn−Teller" (PJT) effect wherein spin−orbit coupling competes with vibronic coupling to lower the energy of the molecule by a distortion from a C_3-symmetric structure.[8] The idealized trigonal Fe(I) geometry created by the [SiP^{iPr}_3]$^-$ ligand leads to a doubly

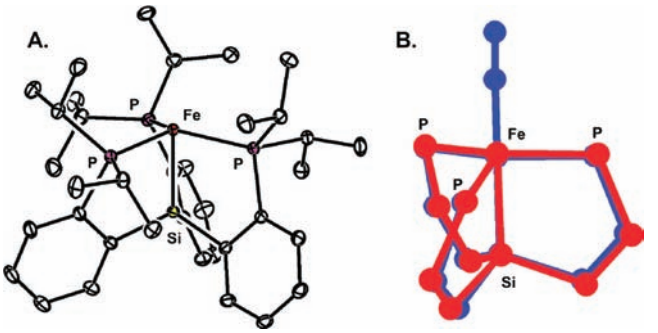

Figure 2. (A) Displacement ellipsoid (50%) representation of **3** obtained from a crystal grown under a H_2 atmosphere. H atoms of SiP^{iPr}_3 have been omitted for clarity. (B) Overlay of the closely related core structures of **2** (blue) and **3** (red).

Table 1. Selected Data for Complexes Discussed in the Text

complex	d_{Fe-Si} (Å)	d_{Fe-P} (Å)	∠PFeP (deg)	μ_{eff} (μ_B)[a]
Fe(N_2) **2**	2.2713(6)	2.2657(5)	111.82(2)	1.90
		2.2841(7)	113.59(2)	
		2.3244(6)	128.64(2)	
Fe(H_2) **3**[b]	2.254(1)	2.2442(9)	113.31(3)	1.88
		2.260(1)	118.07(3)	
		2.2631(9)	122.36(4)	
Fe(H_2) **3**[c]	2.2478(3)	2.2418(3)	113.157(9)	
		2.2577(3)	117.63(1)	
		2.2613(2)	123.16(1)	

[a] Magnetic moments by the Evans method in C_6D_6 at 22 °C. [b] Under vacuum. [c] Under H_2.

degenerate ^{2}E ground state in which the (d_{xy}, $d_{x^2-y^2}$) orbital doublet is triply occupied, and therefore, the complex is subject to a JT distortion. The most obvious distortion in the X-ray structure of **3** (and **2**) is in the P−Fe−P angles, with an increase in one angle from the symmetric value of 120° and a decrease in the other two (e.g., for **3**, P2−Fe−P3 = 123.2° and P1−Fe−P3 ≈ P1−Fe−P2 ≈ 115.4°).

Although the hydrogenic ligand of **3** is not visible by X-ray diffraction (XRD), we directly characterized this ligand by ^{1,2}H ENDOR spectroscopy. Figure 3 displays a part of the 2D field−frequency ^{1}H ENDOR pattern comprising spectra collected across the EPR envelope of **3**. The spectrum collected at g_3 shows a doublet centered at the ^{1}H Larmor frequency that is split by the hyperfine interaction $|A_3(^1H)|$ = 37.8 MHz. The equivalent ^{2}H ENDOR spectrum from [SiP^{iPr}_3]Fe($^2H_2$) (**3′**) shows a corresponding doublet; its splitting, $|A_3(^2H)|$ = 5.6 MHz, matches that of the ^{1}H doublet upon scaling by the respective nuclear g values with a small isotope-effect correction. Likewise, the 2D field−frequency pattern of the ^{2}H ENDOR spectra corresponds to the ^{1}H pattern of Figure 3 (see the SI). The complete 2D pattern is exceptionally well simulated by hyperfine coupling to a *single type* of ^{1}H, with coupling tensor **A** = +[2.3, −40.6, −37.8] MHz, isotropic coupling a_{iso} = −25.4 MHz, and anisotropic dipolar hyperfine coupling tensor **T** = +[27.7, −15.2, −12.4] MHz; the tensor orientation relative to **g** is given by the rotation angles (α, β, γ) = (0, 6, 0). The absolute sign of the ^{1,2}H hyperfine coupling was determined experimentally using the PESTRE technique (see the SI).[9]

The simplest chemical species compatible with a single type of interacting ^{1}H whose Fe−^{1}H vector lies close to $\mathbf{g}_1$ is a neutral

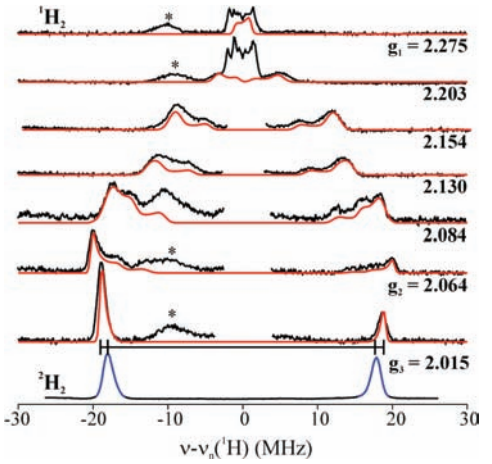

Figure 3. Q-band stochastic 2D field−frequency continuous-wave ENDOR pattern for **3** (black) with simulations of the exogenous "H_2" ^{1}H ENDOR response (red; see the text for details). The corresponding ^{2}H ENDOR spectrum collected from **3**-D_2 at g_3 = 2.015 (blue) is scaled by the ratio of the ^{1}H and ^{2}H nuclear g values. ENDOR responses from ^{31}P of the $[SiP^{iPr}_3]^-$ ligand are indicated by (*).

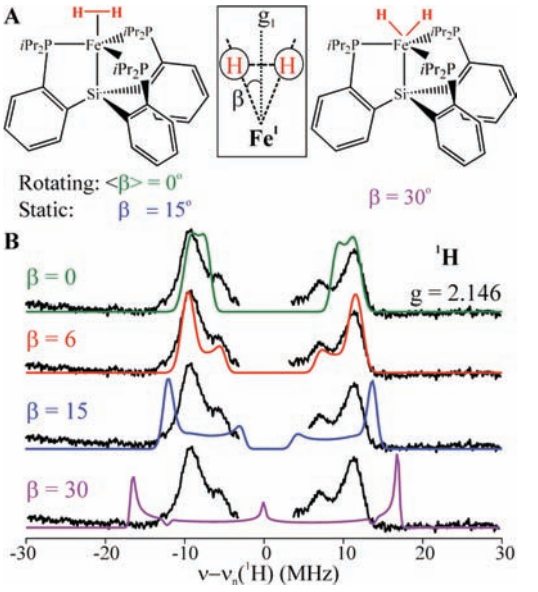

Figure 4. Simulations of ^{1}H ENDOR spectra for models of **3**, for the spectrum at g = 2.146. The simulations are based on the hyperfine tensor determined through a fit to the 2D field−frequency plot of Figure 3 (**A** = [2.3, −40.6, −37.8] MHz) but with the dipolar interaction rotated by the angle β between the H nuclei and the g_1 axis, which is taken to lie along the Fe−Si bond (labeled as "g_1").

complex in which a terminal hydride bound to Fe(I) is generated by heterolytic cleavage of the H_2 molecule with delivery of the proton to the Si of the SiP^{iPr}_3 ligand. However, this model requires cleavage of the Fe−Si bond with rearrangement of the geometry at Si and a substantial increase in d_{Fe-Si} relative to **2**, whereas the crystal structure of **3** reveals a negligible change in d_{Fe-Si} relative to **2** (see above).[10] This conclusion was corroborated by EPR measurements showing that the solution, polycrystalline powder (see the SI), *and* single-crystal forms of **3** have the same **g** tensor[11] and thus the same structure. The ENDOR pattern of Figure 3 must therefore arise from a neutral complex that has been generated by the *addition* of H_2, either in the form of an Fe(I)−H_2 complex or via oxidative addition to an Fe(III) dihydride.

The observed g values provide a powerful argument against the formulation of **3** as an Fe(III) dihydride. The PJT effect predicts that the g values for an Fe(III) d^5 ion must be less than g_e = 2, contrary to observation.[12]

Elimination of the Fe(III) dihydride model for **3** was confirmed by analysis of the ^{1}H ENDOR results. The 2D ENDOR pattern for **3** can be compared with that predicted for this species on the basis of a consensus geometry of similar complexes (d_{H-H} > 1.6 Å; d_{Fe-H} = 1.54 Å; Figure 4).[13] The critical parameter in the ENDOR simulations is the value of the angle β between the g_1 principal axis and the Fe−H vectors. In an Fe(III) dihydride complex, $\beta \geq 30°$. ^{1}H ENDOR simulations using $\beta \approx 30°$ (Figure 4B, β = 30°; also see the SI) showed this to be incompatible with experiment. Figure 4B illustrates this with simulations for a spectrum collected at a field where each component of the doublet observed at g_3 (and g_2) in Figure 3 is split into an intense peak and a less intense "shoulder". The splitting for $\beta \approx 30°$ is far larger than seen experimentally.

Rejection of the assignment of **3** as an Fe(I) monohydride or an Fe(III) dihydride implies by elimination that **3** is an Fe(I)−H_2 adduct. The similarity of the solution NMR and UV−vis data for **2** and **3** are also highly consistent with this notion (see above). The ENDOR simulations further show that even at 2 K, the H_2 of the Fe(I)−H_2 adduct undergoes dynamic reorientation within the ligand-binding pocket of **3**. In a consensus geometry for the Fe(I)−H_2 center (d_{H-H} = 0.85 Å; d_{Fe-H} = 1.62 Å),[14] the H atoms would exhibit a geometrically determined β value of ∼15°. As shown in Figure 4 (also see the SI), the 2D ENDOR pattern of Figure 3 cannot be described by such a static structure. The electron−nuclear dipolar interaction for H_2 must therefore be modulated by rapid reorientation of H_2 about the Fe−H_2 bond axis.

The H_2 cannot undergo rotation that is only weakly hindered by the binding pocket environment because in that case the ground state would correspond to the free-rotor ground rotational state (m = 0).[15] The total wave function of a rotating $^1H_2$ must be antisymmetric with respect to exchange of the two ^{1}H nuclei. For $^1H_2$ bound to the Fe(I) center of a statically distorted **3**, this wave function is the product of the $^1H_2$ rotational and spin functions. The rotor ground state is symmetric with respect to exchange of the two H nuclei (the "para" state) and thus must be associated with the antisymmetric I = 0 total nuclear spin state, which cannot exhibit a ^{1}H ENDOR signal.[16] If **3** instead undergoes a dynamic PJT distortion, the total H_2 wave function would have the vibronic electron−nuclear wave function as an additional factor. For **3** this factor is symmetric with respect to exchange, so the conclusion remains.

Instead, the measurements are probably best understood as a consequence of H_2 tunneling among localized states set up by a strong sixfold barrier associated with rotation of the "dumbell-shaped" H_2 within the threefold-symmetric molecular potential (Figure 5).[5] In this limit, the ^{1}H ENDOR response is allowed, and tunneling would average the dipolar interaction, causing the unique hyperfine axis to lie along the axis of rotation. We attribute the nonzero β to tensor noncollinearity caused by the distortion from trigonal symmetry that is introduced by the PJT effect and observed in the X-ray structure (Table 1).

It is of interest to compare the stable $(SiP^{iPr}_3)Fe^I(H_2)$ complex described here to that assigned as a dihydrogen adduct of Mo(III), "$[HIPTN_3N]Mo^{III}(H_2)$".[6b] In a recent report, it was shown that the latter species undergoes facile heterolytic cleavage of H_2,

dx.doi.org/10.1021/ja207003m |J. Am. Chem. Soc. 2011, 133, 16366–16369

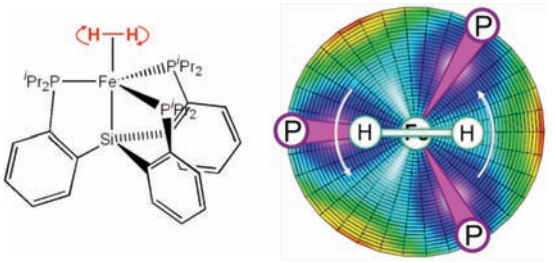

Figure 5. Schematic representation of H_2 hopping/tunneling on the potential energy surface for PJT-distorted **3**.

delivering H^- to Mo to afford $[[HIPTN_3N]Mo^{III}(H)]^-$ and H^+, with the H^+ presumably delivered to sacrificial $[HIPTN_3N]^{3-}$ at reduced temperature.[6c] In contrast, the Si atom of the $(SiP^{iPr}_3)Fe$ scaffold is insufficiently basic to accept H^+ from the coordinated H_2, thus stabilizing the H_2 adduct complex **3** against heterolytic cleavage. The stability of H_2 bound to the "$(SiP^{iPr}_3)Fe$" scaffold also extends to its corresponding cation, "$(SiP^{iPr}_3)Fe^{+}$". Treating previously reported $S = 1$ $\{(SiP^{iPr}_3)Fe(N_2)\}\{BAr^F_4\}$ (**4**) with H_2 reversibly generates what we have assigned as the $S = 1$ complex $\{(SiP^{iPr}_3)Fe(H_2)\}\{BAr^F_4\}$ (**5**) (Scheme 1). Complex **5** is EPR/ENDOR-silent because of its integer-spin triplet state, but solution NMR and UV−vis data (see the SI) provide evidence for a species that is highly similar to the cationic N_2 adduct **4**. Moreover, addition of an exogenous base (e.g., N^iPr_2Et) to **5** under N_2 cleanly effects heterolytic cleavage, affording the neutral Fe(II) complex $(SiP^{iPr}_3)Fe(N_2)(H)$ (**6**) (Scheme 1).

In summary, the mononuclear $S = {}^1/_2$ $Fe^I(H_2)$ adduct complex **3** provides a highly unusual example of a well-characterized open-shell metal complex that binds dihydrogen as a ligand. Combined XRD, EPR, and ENDOR data are consistent with a PJT-distorted d^7 configuration and a H_2 ligand that at 2 K tunnels among the energetic minima created by the Fe−P bonds. The $S = {}^1/_2$ title complex $(SiP^{iPr}_3)Fe(H_2)$ can be formally oxidized to its $S = 1$ cation, $\{(SiP^{iPr}_3)Fe(H_2)\}^+$, and the latter species binds H_2 as an intact ligand that is subject to heterolytic cleavage upon addition of exogenous base.

■ ASSOCIATED CONTENT

Supporting Information. Experimental procedures, characterization and crystallographic data. This material is available free of charge via the Internet at http://pubs.acs.org.

■ AUTHOR INFORMATION

Corresponding Author
bmh@northwestern.edu; jpeters@caltech.edu

Present Addresses
[§]Department of Chemistry, School of Molecular Science, Korea Advanced Institute of Science and Technology, Daejon, Republic of Korea.

Author Contributions
[‖]These authors contributed equally.

■ ACKNOWLEDGMENT

We acknowledge the NIH (GM-070757 to J.C.P.; HL 13531 to B.M.H.). We thank Prof. Harden McConnell for insightful suggestions about low-temperature dynamics. Dr. Peter Müller provided assistance with XRD analyses. Professor George R. Rossman provided access to a near-IR spectrometer. Henry Fong probed the deprotonation of **5**.

■ REFERENCES

(1) (a) Tard, C.; Pickett, C. J. *Chem. Rev.* **2009**, *109*, 2245. (b) Gloaguen, F.; Rauchfuss, T. B. *Chem. Soc. Rev.* **2009**, *38*, 100. (c) Vincent, K. A.; Parkin, A.; Armstrong, F. A. *Chem. Rev.* **2007**, *107*, 4366.

(2) (a) Smith, J. M.; Lachiotte, R. J.; Pittard, K. A.; Cundari, T. R.; Rodgers, K. R.; Lukat-Rodgers, G.; Lachiotte, R. J.; Flaschenriem, C. J.; Vela, J.; Holland, P. L. *J. Am. Chem. Soc.* **2006**, *123*, 756. (b) Holland, P. L. *Can. J. Chem.* **2005**, *83*, 296.

(3) (a) Betley, T. A.; Peters, J. C. *J. Am. Chem. Soc.* **2004**, *126*, 6252. (b) Mankad, N. P.; Whited, M. T.; Peters, J. C. *Angew. Chem., Int. Ed.* **2007**, *46*, 5768. (c) Brown, S. D.; Betley, T. A.; Peters, J. C. *J. Am. Chem. Soc.* **2003**, *125*, 322.

(4) (a) Lee, Y.; Mankad, N. P.; Peters, J. C. *Nat. Chem.* **2010**, *2*, 558. (b) Whited, M. T.; Mankad, N. P.; Lee, Y.; Oblad, P. F.; Peters, J. C. *Inorg. Chem.* **2009**, *48*, 2507. (c) Lee, Y.; Peters, J. C. *J. Am. Chem. Soc.* **2011**, *133*, 4438.

(5) Kubas, G. J. *Chem. Rev.* **2007**, *107*, 4152.

(6) For the few cases where H_2 has been suggested to be coordinated to an open-shell metal center, see: (a) Hetterscheid, D. G. H.; Hanna, B. S.; Schrock, R. R. *Inorg. Chem.* **2009**, *48*, 8569. (b) Kinney, R. A.; Hetterscheid, D. G. H.; Schrock, R. R.; Hoffman, B. M. *Inorg. Chem.* **2010**, *49*, 704. (c) Bart, S. C.; Lobkovsky, E.; Chirik, P. J. *J. Am. Chem. Soc.* **2004**, *126*, 13794. (d) Baya, M.; Houghton, J.; Daran, J.-C.; Poli, R.; Male, L.; Albinati, A.; Gutman, M. *Chem.—Eur. J.* **2007**, *13*, 5347.

(7) (a) Heinekey, D. M.; Lledós, A.; Lluch, J. *Chem. Soc. Rev.* **2004**, *33*, 175. (b) Jessop, P. G.; Morris, R. H. *Coord. Chem. Rev.* **1992**, *121*, 155. (c) Morris, R. H. *Coord. Chem. Rev.* **2008**, *252*, 2381.

(8) (a) Bersuker, I. B. *The Jahn−Teller Effect*, 1st ed.; Cambridge University Press: Cambridge, U.K., 2006; (b) McNaughton, R. L.; Roemelt, M.; Chin, J. M.; Schrock, R. R.; Neese, F.; Hoffman, B. M. *J. Am. Chem. Soc.* **2010**, *132*, 8645.

(9) Doan, P. E. *J. Magn. Reson.* **2011**, *208*, 76.

(10) DFT calculations showed that an isomer with one H atom on Si and on Fe, $(HSiP^{iPr}_3)Fe(H)$, is energetically inaccessible relative to $(SiP^{iPr}_3)Fe(H_2)$ or $(SiP^{iPr}_3)Fe(H)_2$ isomer.

(11) Gurbiel, R. J.; Bolin, J. T.; Ronco, A. E.; Mortenson, L.; Hoffman, B. M. *J. Magn. Reson.* **1991**, *91*, 227.

(12) Ammeter, J. H. *J. Magn. Reson.* **1978**, *30*, 299.

(13) Cambridge Structural Database (CSD).

(14) Bruno, I. J.; Cole, J. C.; Edgington, P. R.; Kessler, M.; Macrae, C. F.; McCabe, P.; Pearson, J.; Taylor, R. *Acta Crystallogr.* **2002**, *B58*, 389.

(15) McConnell, H. M. *J. Chem. Phys.* **1958**, *29*, 1422.

(16) Eckert, J.; Kubas, G. J. *J. Phys. Chem.* **1993**, *97*, 2378.